

DETERMINATION OF WEATHERING TREND USING SEISMIC REFLECTION DATA OF SOUTH-WEST NIGER DELTA BASIN

*Sofolabo O. A.¹, Ekine A. S.² and Ehirim C.³

^{1,2,3} - Department of Physics

University of Port Harcourt, Rivers State

(aosofolabo1@yahoo.com, asekine2001@yahoo.com,)

Received: 6-7-11

Accepted: 25-5-11

ABSTRACT

A procedure for delineating the weathering trend along a seismic line from reflection data of a study area OML-39 of South-West Niger Delta Basin is presented. Data obtained from SP 422 – 500, Line 105 of the OML 39 of the Okuibome prospect, Delta State, South West Niger Delta Area are presented as a case study. A plot of first break time at a geophone station versus the geophone take-off distance from a seismic shot is made for total of 40 shots, using first breaks time for 14 active traces per shot point. From these plots, the elevation velocity (consolidated layer velocity) for the different shot points were obtained, which ranges from 1642ms^{-1} at the western part of the field to 1862ms^{-1} at the eastern part with an average value of 1724ms^{-1} across the line profile. A datum surface was assumed, and a plot of both the shots and geophones elevation above the datum surface along the line gives the surface topography of the area. Subsequently, the weathering thickness along the line was obtained using the elevation velocity obtained, shot depth, weathering velocity and calculated modified intercept time T_{mod} of the first break and take off distance plots for each of the shot points. With a weathering velocity of 500ms^{-1} (supplied from uphole survey of the area), the weathering thickness obtained for the area along the line ranges from 35.46m in the low side to 50.87m in the high side, with an average thickness of 42.66m for the study area along the line, the variation of the weathering thickness along the line is significant. By plotting the weathering thickness, shot and geophone elevation at the stations, the weathering trend of the study area was delineated. The determination of the weathering thickness at a shot point requires consideration of the shot and geophone configurations which have to be modified in the computation to suit the actual field situations. From the results obtained, the thickness is highly influenced by the topography along the area, thus weathering thickness along the line of the study area is topography dependent.

Key words: Weathering trend, Weathering thickness, Weathering layer, First break time, Take-off distance, Intercept time, Reflection data and Low-velocity layers.

INTRODUCTION

The existence of a near surface layer with low velocity characteristics has been recognized in seismic work for several years, this layer being almost universally present irrespective of surface deposits. This layer is capable of absorbing higher frequency signals and releasing lower ones. As a result, when shots are taken within this layer, they tend to propagate with weaker frequency and this reduces quality of the data

obtained from such shots. It is therefore necessary that shots be taken below the weathering layer in order to improve data quality. Other characteristics of this layer include heavy ground roll, reverberation and introduction of delays to seismic signals. Geophysical weathering (seismic weathering) also known as low-velocity layer (LVL) is usually different from geologic weathering (which is as a result of rock decomposition).

This layer is usually the portion of the earth where air rather than water fills the pore spaces of rocks and the unconsolidated earth. Frequently the base of the weathering is the water table. Sometimes the weathering velocity is gradational or sharply layered (Sheriff, 2006).

Uphole survey (which is a refraction survey) is the most commonly used survey for the determination of weathering thickness in a seismic data acquisition work. This survey however is very costly to operate and as a result it is seldom carried out at short distances along a seismic line (NNPC-IDSL, 1992). Thus, this survey cannot be used to give accurate representation of weathering trend in the area of survey. In seismic reflection data acquisition work, shots are taken at every shot point which is separated only by short intervals along the seismic line. Thus, if weathering thickness can be determined at every shot point along a seismic line, a better representation of the weathering trend can be given.

Thus, a practical procedure for determining or delineating the weathering trend of the study area from seismic reflection data is presented.

Reflection Data Acquisition Principles

Seismic reflection survey is conducted in an area to map subsurface geological structures by acquiring seismic data of the subsurface (Toksovet, 1987). The survey involves the initiation of shock wave of acoustic energy into the subsurface of the earth. When a shock wave of acoustic energy is initiated into the earth, it travels down with the velocity of the various layers of the earth, and after its reflection from the various boundaries, it returns to the surface where it is picked up by an acoustic sensor planted on the earth's surface (Telford et al, 1982). The reflections from the various horizons constitute the seismic data required, whose time of arrival, amplitude and character contain information regarding subsurface geological surfaces.

Field Layout for the Data Acquisition

The Okuibome Prospect where the data for this study was acquired is a 2-D Prospect, an SPDC OML in Niger Delta Area (Delta State). The shots (given in even numbers) are 50m apart while the geophone stations (given in odd numbers) are 25m apart. The short are pattern shots of five (5) shot holes per shot point, 3m deep with 5m interspacing. Ten (10) geophone jugs, 2.5m apart, are used per geophone station and each shot is taken into a total of 120 geophone stations, covering a total distance of 2.975km. A schematic diagram of the shot point and geophones arrays is shown in Fig. 1

MATERIALS AND METHODS

The Data

The data for the study include (an SPDC OML 39 Prospect data, South –East Niger Delta Basin, Delta State):

1. Reflection monitor records for shot points (422 – 500) – First Break Data (Appendix A, Table 1).
2. Surface elevation of shot and geophones (Appendix B, Table 2).
3. Shot depth (3m)
4. Instrument delay (5mms).
5. Weathering velocity (500 msec^{-1} obtained from LVL survey).

Data Analysis

Picking of time breaks/plotting

The first break is the first pick-up time recorded by a geophone. For each shot, first breaks are picked starting from the sixth active trace from the shot point. The first three traces for each shot are normally regarded as dead traces, these traces are the direct arrivals from the shot depth point and are mostly not reflected. All other arrivals are generally active, thus the first active trace or arrival from a shot point is the 4th trace which is 87.5m from the shot while the sixth active trace being the 9th trace which is 212.5m from the shot (Fig. 2).

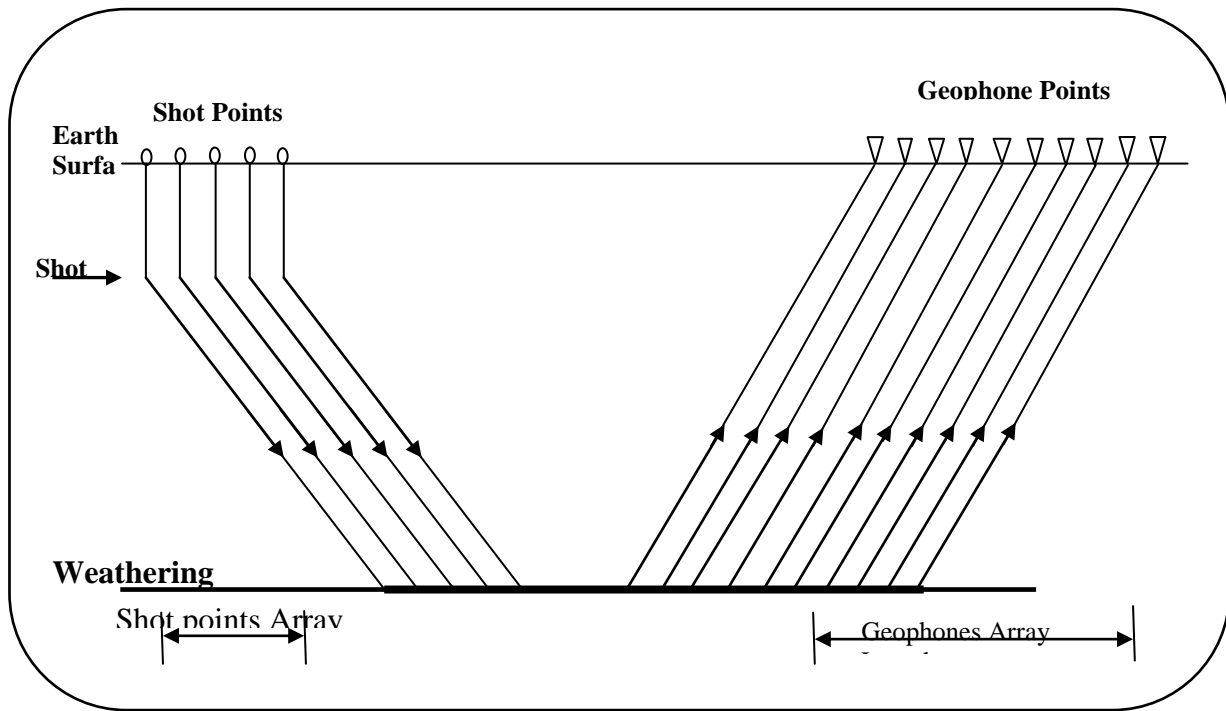


Fig. 1: Schematic Diagram of Shot and Geophone Array

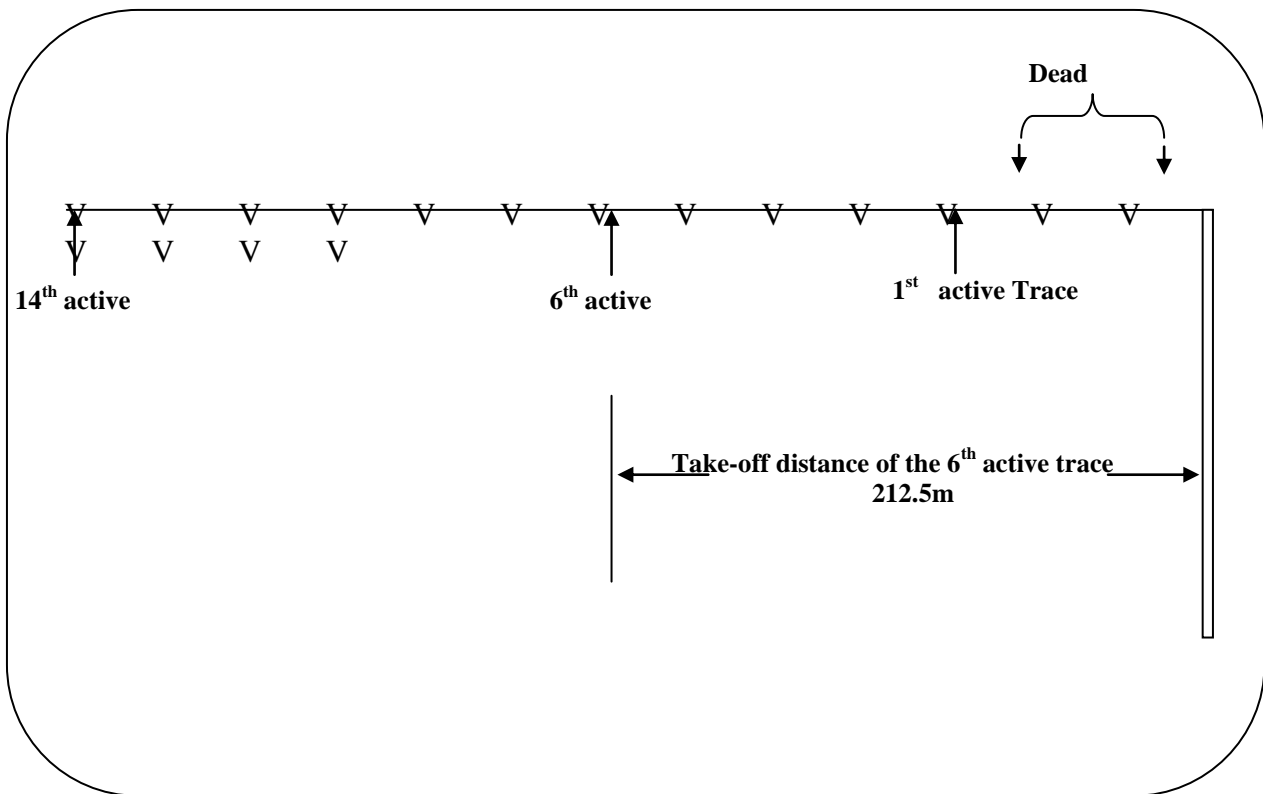


Fig. 2: Field layout and time pick for shot point

Starting from the sixth active trace, the picking is done for the first 14 active traces for every shot (out of the total of 120 traces for the shot for a short interval spatial coverage, thus making the survey cost effective), the 14th active trace being 325m from the shot point (Table 3).

A plot of the first break versus the take-off distance of the traces from the shot point is then made and thereafter, the best fit curve is drawn through the points whose inverse slope gives the elevation velocity for that particular shot point (Fig. 3).



Fig. 3: Time break versus trace offset plot for a single shot

Computation of the Intercept time (T_i)

To compute the intercept time for a shot, the curve is extrapolated (Fig. 3) to the time axis, which is the shot point (SP) to read off the intersection on the time axis.

Ordinarily if only a single geophone jug (instead of array of geophone jugs) and a single shot hole (instead of pattern holes) had been used at the geophone and shot stations respectively, then the point of intersection of this curve on the time axis

would give the intercept time, T_i . But because of the array of geophone jugs and shot holes at the geophone and shot stations, (a 2-D survey required an area investigation, which is not possible with single shot hole pattern), thus modification is made to take into account the actual configuration of the shots and geophones.

Consider a single shot of five shot holes and a single trace (or geophone station) of ten jugs as shown in Fig. 4.

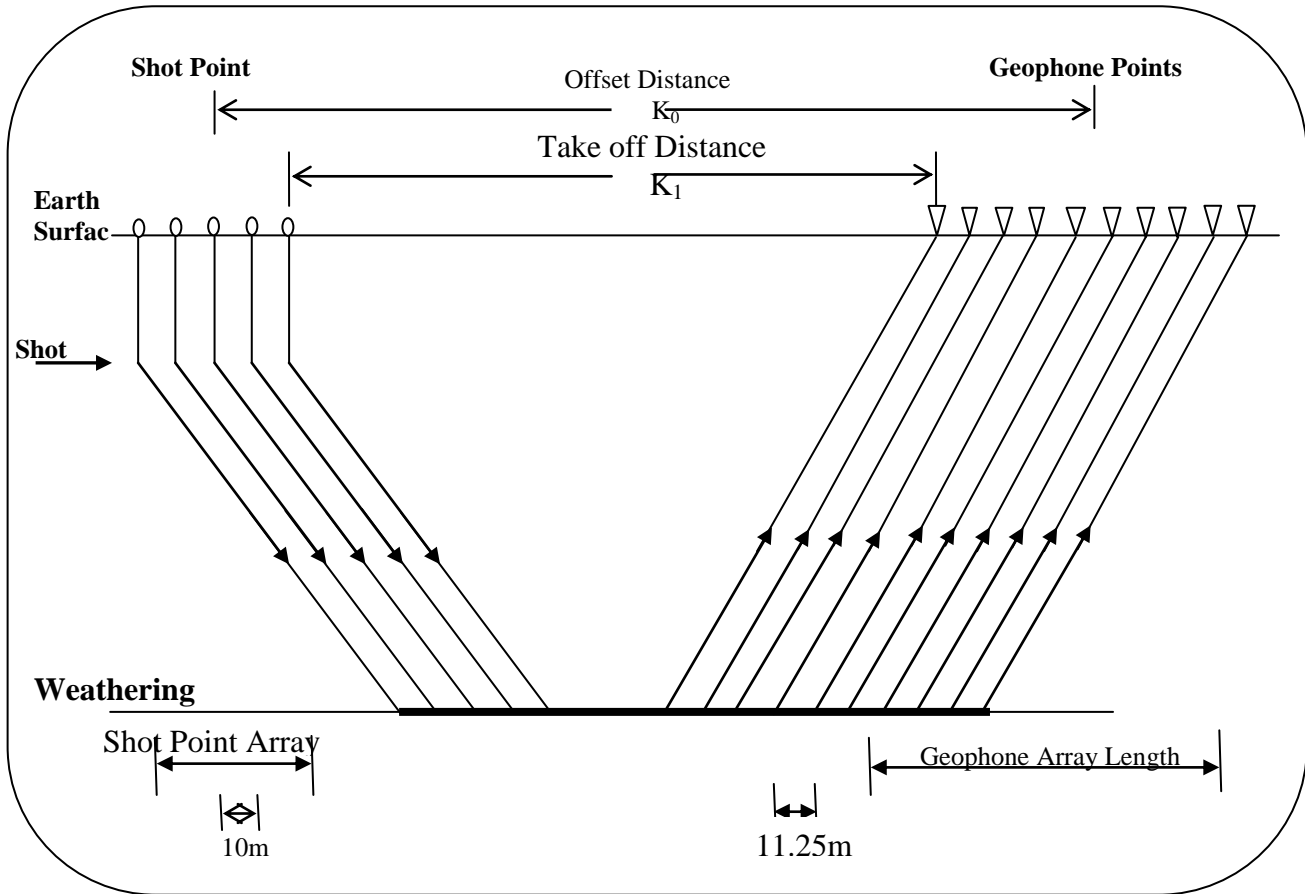


Fig. 4: Field Set Up for Reflection Data Acquisition

The distance K_0 is the offset distance of the shot and geophone stations, i.e., the distance between the mid points of the shot array and the geophone array. For example, this distance for the sixth active trace is 212.5m. However, the distance K_1 , which is between the last shot hole and the first geophone jug from the shot is practically the distance of interest, in the determination of weathering depth, obtained for a pattern shot and array of geophones. This distance is obtained by the relation (May, et al, 1981).

$$\begin{aligned}
 K_1 &= \frac{1}{2} (\text{geophone array length}) + \frac{1}{2} (\text{shot array length}) \dots\dots\dots 1 \\
 &= \frac{1}{2} (25) + \frac{1}{2} (20) \\
 &= 11.25 + 10 = 21.25\text{m}
 \end{aligned}$$

To compute the intercept time, therefore, the position of the shot is shifted by this amount (21.25m) and thereafter, the

intersection on this new position is read as the modified intercept, T_{mod} on the time axis. This shift, S , is synonymous to subtracting the distance K_1 from the take-off distance, K_1 of every trace from the shot (Table 3). That is,

$$\begin{aligned}
 S &= K_0 - K_1 \dots\dots\dots 2 \\
 &= K_0 - 21.25\text{m}
 \end{aligned}$$

For example, for the sixth active trace of every shot (Table 3) will be at

$$\begin{aligned}
 S &= 212.5 - 21.25 \\
 &= 191.25\text{m}
 \end{aligned}$$

Therefore, 191.25m will be the actual take off distance of the sixth trace upon consideration of the shot and geophone array lengths (Table 4) and Fig. 3 will then take the form of Fig. 5 below.

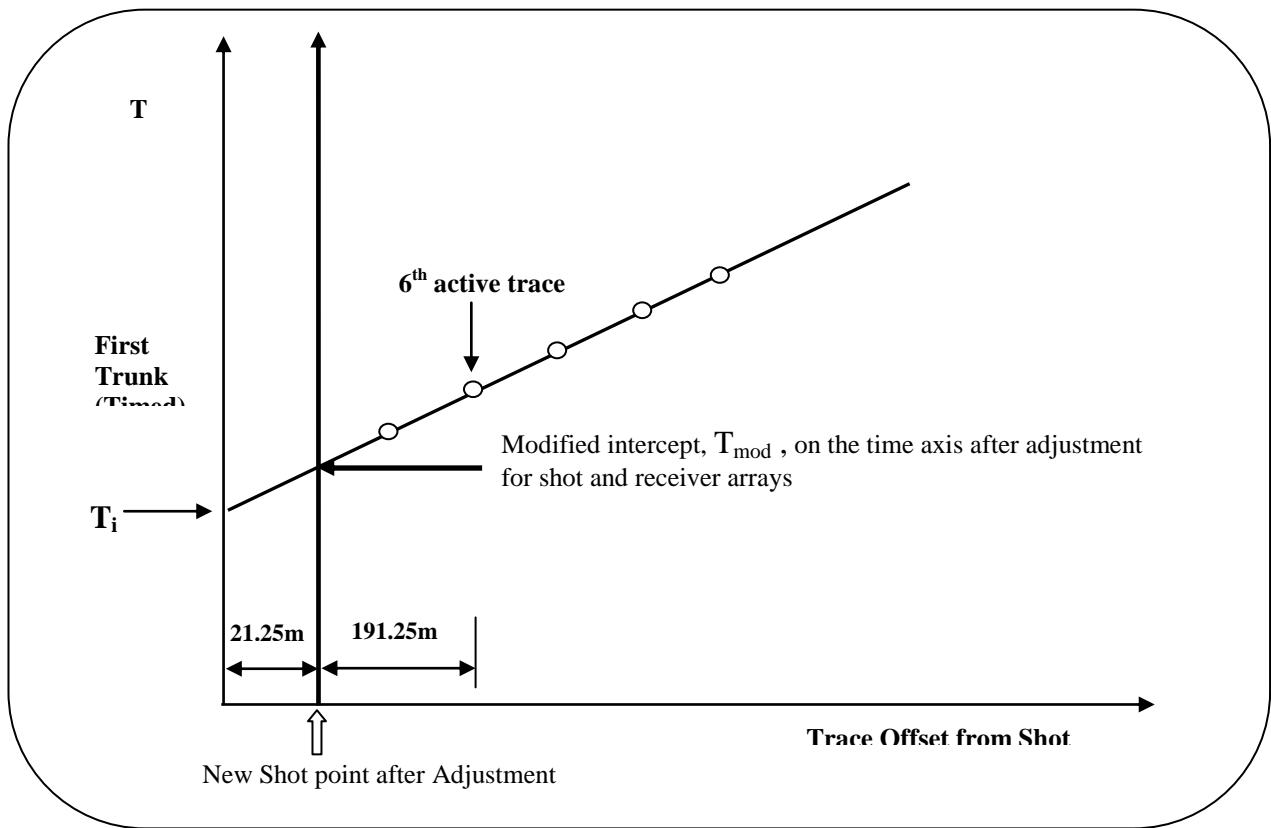


Fig. 5: Intercept time computation from first break – trace offset plot.

Without instrument delay, this modified intercept, T_{mod} , after the adjustment would give the actual intercept time T_i , for the shot. But with instrument delay, i_d , the actual intercept is obtained by the following equation.

$$T_i = (T_{mod} - i_d) \dots \dots \dots 3$$

Since the instrument delay is 5ms (as obtained during acquisition (supplied) mentioned earlier), the intercept time becomes:

$$T_i = (T_{mod} - 5) \text{ ms} \dots \dots \dots 4$$

For example, at SP 422 (Table 5) intersection time on the time axis before adjustment is 122ms (Appendix D). But after adjustment, $T_{mod} = 135$ ms thus the new intercept time T_i is 130 ms (Table 5).

Determination of the weathering depth

The determination of the weathering trend for the study area from reflection seismic is assumes a single layer of weathering, since a single line seismic data were used, thus dip and far offset

distance is not considered and from general principles, the total travel time of seismic waves for a shot located in the weathering layer is given by the relation (Hubral, et al, 1980):

$$T = \frac{X}{V_e} + \frac{2d_w \cos i}{V_w} + \frac{d_s}{2}$$

..... 5

Where T = Total travel time from shot to receiver

X = shot – receiver offset

d_w = depth of weathering

V_e = elevation Velocity

V_w = weathering velocity (500ms^{-1})

d_s = depth of shot (3m)

i = incidence angle of ray path

At zero offset, $T = T_i$ ($X = 0$), the equation reduces to

$$T_i = \frac{2d_w \cos i}{V_w} + \frac{d_s}{2}$$

..... 6

Rearranging,

$$d_w = \frac{T_i V_w}{2 \cos i} + \frac{d_s}{2}$$

..... 7

Where,

$$\cos i = \sqrt{1 - \frac{V_w^2}{V_e^2}}$$

..... 8

Equation 7 gives the weathering depth at each shot point (Appendix C and Table 5). The elevation velocity, V_e , used in this equation is the average of all elevation velocities computed

from the inverse slope of each curve along the seismic line (Appendix D, Fig 7a-h), with layer velocity

ranging from 1642ms^{-1} to 1862ms^{-1} with an average of $1,724 \text{ms}^{-1}$ for this study.

Preparation of the Weathering Profile

To determine the weathering trend along the seismic line, a datum surface is assumed and the surface elevation of shots and geophones along the line is plotted above this datum surface directly on top of the stations. By joining these points, surface topography along the seismic line is obtained. Using the same scale, the depth of weathering at each shot point is then plotted and joined to delineate the weathering trend along the line as shown in Figure 6 and Table 6.

RESULTS**TABLE 1: First Break Data (SPDC) - Reflection Monitor Data**

First Break Time (millisecond - msec)														
SP No	1	2	3	4	5	6	7	8	9	10	11	12	13	14
422	242	260	271	290	302	318	330	342	360	372	388	400	418	430
424	248	260	276	290	300	317	331	343	360	372	390	401	419	431
426	249	261	274	290	304	320	333	346	362	380	390	404	420	433
428	250	260	277	290	306	320	333	350	360	379	392	406	422	440
430	250	261	280	292	308	322	337	352	364	380	391	410	420	430
432	250	266	280	296	310	322	340	352	370	382	397	412	424	442
434	250	264	280	298	308	326	338	351	366	380	394	410	424	440
436	254	269	284	300	312	327	340	356	370	386	400	414	427	440
438	250	270	282	298	311	324	340	353	370	381	400	411	429	441
440	250	270	284	300	314	330	344	358	371	388	401	416	431	448
442	254	270	284	300	314	330	342	360	371	389	402	417	433	447
444	257	272	288	300	316	330	341	360	376	390	407	420	434	450
446	259	274	285	300	316	330	349	360	378	390	408	420	435	450
448	260	274	290	304	320	335	350	362	378	395	410	426	438	450
450	260	276	292	306	321	340	353	368	384	396	410	423	440	456
452	263	280	296	314	326	340	354	370	382	397	412	426	440	456
454	266	280	297	310	326	340	354	369	385	399	414	430	442	458
456	270	284	300	315	329	340	359	369	384	400	418	434	441	460
458	270	283	297	312	328	341	358	372	387	400	414	430	444	460
460	270	285	301	318	329	346	360	375	390	404	420	432	450	461
462	275	290	306	320	335	349	365	379	394	403	419	436	447	465
464	278	292	310	320	336	353	367	382	394	410	425	443	455	470
466	280	294	310	324	340	354	368	386	400	414	430	443	458	472
468	293	308	320	324	349	361	380	393	409	424	439	455	465	480
470	281	291	310	326	340	353	370	386	400	414	430	444	459	474
472	285	300	313	329	345	360	374	388	405	420	432	444	462	476
474	289	302	317	332	346	362	376	390	406	420	434	450	463	480
476	290	304	320	334	350	362	377	394	410	420	435	450	463	474
478	290	303	320	337	349	364	380	392	406	420	436	450	464	478
480	291	307	322	337	351	366	381	394	410	426	442	454	469	482
482	297	311	323	339	351	366	381	397	410	422	440	454	470	481
484	299	313	327	340	352	370	384	398	412	430	445	454	473	486
486	300	314	330	341	360	370	389	401	413	430	440	460	473	489
488	300	314	330	343	360	372	388	400	416	432	444	460	470	469
490	300	316	330	346	357	370	385	402	420	433	445	454	470	485
492	300	316	330	341	360	374	392	402	415	430	446	460	475	489
494	300	316	331	345	361	374	391	401	420	433	444	461	474	494
496	301	319	334	350	364	377	393	408	424	434	450	466	480	491
498	308	320	335	350	366	378	396	410	425	439	454	469	484	490
500	308	323	340	353	366	384	396	411	427	440	455	469	483	495

TABLE 2: Elevation Data of Shot points and Geophones (SPDC)

Shot No	Geophone No	Elevation of Shot (M)	Elevation of Geophone (M)	Shot Depth (M)	Shot No	Geophone No	Elevation of Shot (M)	Elevation of Geophone (M)	Shot Depth (M)
422		92.5		3	470		121.0		3
	423		93.2			471		121.8	
424		93.6		3	472		122.4		3
	425		94.0			473		122.8	
426		94.5		3	474		123.7		3
	427		94.9			475		124.1	
428		95.7		3	476		124.9		3
	429		96.0			477		125.8	
430		96.4		3	478		126.4		3
	431		96.5			479		126.9	
432		97.5		3	480		127.6		3
	433		98.0			481		127.9	
434		98.6		3	482		128.5		3
	435		98.1			483		129.2	
436		99.6		3	484		129.6		3
	437		100.2			485		130.2	
438		101.0		3	486		130.7		3
	439		101.4			487		131.2	
440		102.0		3	488		131.7		3
	441		102.2			489		132.0	
442		103.0		3	490		132.7		3
	443		103.8			491		133.0	
444		104.2		3	492		133.7		3
	445		105.1			493		133.7	
446		105.6		3	494		134.3		3
	447		106.2			495		134.7	
448		106.7		3	496		135.1		3
	449		107.4			497		135.6	
450		108.3		3	498		136.0		3
	451		108.6			499		136.6	
452		109.2		3	500		137.8		3
	453		109.7						
454		110.6		3					
	455		111.2						
456		111.7		3					
	457		112.5						
458		113.3		3					
	459		114.0						
460		114.5		3					
	461		115.5						
462		115.8		3					
	463		116.4						
464		117.3		3					
	465		117.7						
466		118.5		3					
	467		119.2						
468		119.8		3					
	469		120.5						

TABLE 3: Active trace offset distance and take-off distance

S/No	Traces	Status	Trace offset layout distance (m)	Trace take-off distance from Shot point(m)	Actual take-off distance(m)
1	1 st	Dead	25	-	-
2	2 nd	Dead	50	-	-
3	3 rd	Dead	75	-	-
4	4 th	Active	100	87.5	66.25
5	5 th	Active	125	112.5	91.25
6	6 th	Active	150	137.5	116.25
7	7 th	Active	175	162.5	141.25
8	8 th	Active	200	187.5	166.25
9	9 th	Active	225	212.5	191.25
10	10 th	Active	250	237.5	216.25
11	11 th	Active	275	262.5	241.25
12	12 th	Active	300	287.5	266.25
13	13 th	Active	325	312.5	291.25
14	14 th	Active	350	337.5	316.25
15	15 th	Active	375	362.5	341.25

TABLE 4: Active trace take off distance and travel time (Arrival time)

Take-off distance (m)	87.5m	112.5m	137.5m	162.5m	187.5m	212.5m	237.5m	262.5m	287.5m	312.5m	337.5m
Arrival Time Shot point	1 st Active Trace (ms)	2 nd Active Trace (ms)	3 rd Active Trace (ms)	4 th Active Trace (ms)	5 th Active Trace (ms)	6 th Active Trace (ms)	7 th Active Trace (ms)	8 th Active Trace (ms)	9 th Active Trace (ms)	10 th Active Trace (ms)	11 th Active Trace (ms)
422	290	302	318	330	342	360	372	388	400	418	430
424	290	300	317	331	343	360	372	390	401	419	431
426	290	304	320	333	346	362	380	390	404	420	433
428	290	306	320	333	350	360	379	392	406	422	440
430	292	308	322	337	352	364	380	391	410	420	430
432	296	310	322	340	352	370	382	397	412	424	442
434	298	308	326	338	351	366	380	394	410	424	440
436	300	312	327	340	356	370	386	400	414	427	440
438	298	311	324	340	353	370	381	400	411	429	441
440	300	314	330	344	358	371	388	401	416	431	448
442	300	314	330	342	360	371	389	402	417	433	447
444	300	316	330	341	360	376	390	407	420	434	450
446	300	316	330	349	360	378	390	408	420	435	450
448	304	320	335	350	362	378	395	410	426	438	450
450	306	321	340	353	368	384	396	410	423	440	456
452	314	326	340	354	370	382	397	412	426	440	456
454	310	326	340	354	369	385	399	414	430	442	458
456	315	329	340	359	369	384	400	418	434	441	460
458	312	328	341	358	372	387	400	414	430	444	460
460	318	329	346	360	375	390	404	420	432	450	461
462	320	335	349	365	379	394	403	419	436	447	465
464	320	336	353	367	382	394	410	425	443	455	470
466	324	340	354	368	386	400	414	430	443	458	472
468	324	349	361	380	393	409	424	439	455	465	480
470	326	340	353	370	386	400	414	430	444	459	474
472	329	345	360	374	388	405	420	432	444	462	476
474	332	346	362	376	390	406	420	434	450	463	480
476	334	350	362	377	394	410	420	435	450	463	474
478	337	349	364	380	392	406	420	436	450	464	478
480	337	351	366	381	394	410	426	442	454	469	482
482	339	351	366	381	397	410	422	440	454	470	481
484	340	352	370	384	398	412	430	445	454	473	486
486	341	360	370	389	401	413	430	440	460	473	489
488	343	360	372	388	400	416	432	444	460	470	469
490	346	357	370	385	402	420	433	445	454	470	485
492	341	360	374	392	402	415	430	446	460	475	489
494	345	361	374	391	401	420	433	444	461	474	494
496	350	364	377	393	408	424	434	450	466	480	491
498	350	366	378	396	410	425	439	454	469	484	490
500	353	366	384	396	411	427	440	455	469	483	495

TABLE 5: Determination of Intercept time and Weathering depth along Shot point

S/No	Shot Point (SP)	Curve Intercept Time- T_{mod} (ms)	Instrument Delay Time I_d (ms)	Adjusted Intercept Time $T_i = T_{mod} - I_d$ (ms)	Weathering Depth- D_w (m)
1	422	135	5	130	35.46
2	424	139	5	134	36.50
3	426	139	5	134	36.50
4	428	140	5	135	36.77
5	430	142	5	137	37.29
6	432	139	5	134	36.50
7	434	138	5	133	36.24
8	436	146	5	141	38.33
9	438	144	5	139	37.81
10	440	143	5	138	37.55
11	442	142	5	137	37.29
12	444	146	5	141	38.33
13	446	147	5	142	38.59
14	448	148	5	143	38.86
15	450	154	5	140	38.07
16	452	152	5	147	39.90
17	454	153	5	148	40.16
18	456	158	5	153	41.47
19	458	158	5	153	41.47
20	460	157	5	152	41.21
21	462	163	5	158	42.77
22	464	166	5	161	43.56
23	466	168	5	163	44.08
24	468	183	5	178	48.00
25	470	167	5	162	43.82
26	472	172	5	167	45.13
27	474	176	5	171	46.17
28	476	178	5	173	46.69
29	478	177	5	172	46.43
30	480	178	5	173	46.69
31	482	177	5	172	46.43
32	484	187	5	182	49.04
33	486	186	5	181	48.78
34	488	186	5	181	48.78
35	490	186	5	181	48.78
36	492	184	5	179	48.26
37	494	186	5	181	48.78
38	496	188	5	183	49.31
39	498	190	5	185	49.83
40	500	194	5	189	50.87

Table 6: Shot point, Geophone Elevation, Shot Elevation and Weathering Depth above the datum Surface of the Area

Shot Point	Geophone Elevation (m)	Shot Elevation (m)	Weathering Depth (m)
422	93.2	92.5	35.46
424	94	93.6	36.5
426	94.9	94.5	36.5
428	96	95.7	36.77
430	96.5	96.4	37.29
432	98	97.5	36.5
434	98.1	98.6	36.24
436	100.2	99.6	38.33
438	101.4	101	37.81
440	102.2	102	37.55
442	103.8	103	37.29
444	105.1	104.2	38.33
446	106.2	105.6	38.59
448	107.4	106.7	38.86
450	108.6	108.3	38.07
452	109.7	109.2	39.9
454	111.2	110.6	40.16
456	112.5	111.7	41.47
458	114	113.3	41.47
460	115.5	114.5	41.21
462	116.4	115.8	42.77
464	117.7	117.3	43.56
466	119.2	118.5	44.08
468	120.5	119.8	48
470	121.8	121	43.82
472	122.8	122.4	45.13
474	124.1	123.7	46.17
476	125.8	124.9	46.69
478	126.9	126.4	46.43
480	127.9	127.6	46.69
482	129.2	128.5	46.43
484	130.2	129.6	49.04
486	131.2	130.7	48.78
488	132	131.7	48.78
490	133	132.7	48.78
492	133.7	133.7	48.26
494	134.7	134.3	48.78
496	135.6	135.1	49.31
498	136.6	136	49.83
500		137.8	50.87

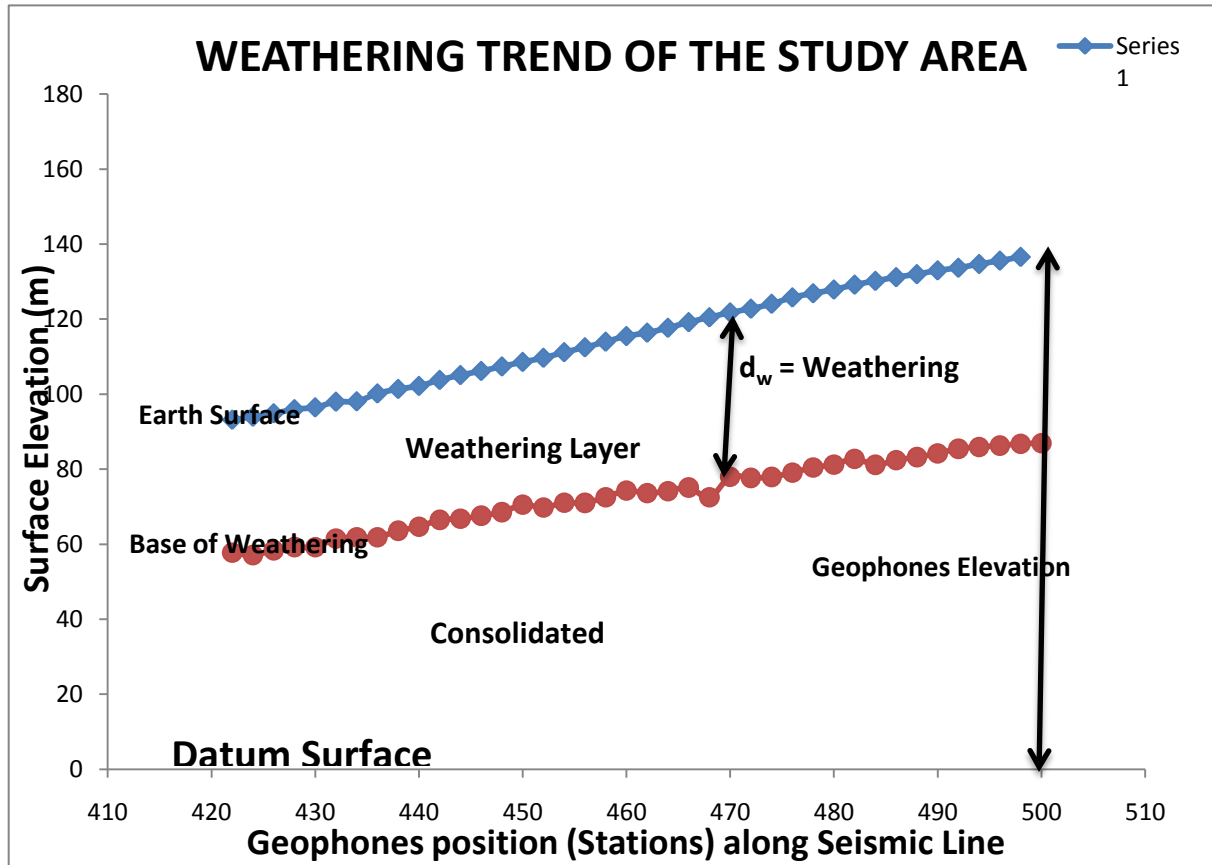


Fig. 6: The Profile of the Weathering Layer of the Study Area

Calculation of weathering depth along shot and geophone elevation points along seismic Line using the relation

$$d_w = \frac{T_i V_w}{2 \cos i} + \frac{d_s}{2}$$

and

$$\cos i = \sqrt{1 - \frac{V_w^2}{V_e^2}} = \sqrt{1 - \frac{(500)^2}{(1724)^2}} = \sqrt{1 - 0.9159} = 0.95702$$

Where $d_s = 3\text{m}$, $V_e = 1724\text{ms}^{-1}$, $V_w = 500\text{ms}^{-1}$.

Thus at SP 422:

$$d_w = \frac{0.13 \times 500}{2(0.9570)} + \frac{3}{2} = 33.956 + 1.5 = 35.46$$

m

SP 424:

$$d_w = \frac{0.134 \times 500}{2(0.9570)} + \frac{3}{2} = 35.004 + 1.5 = 36.5 \text{ m}$$

SP 426:

$$d_w = \frac{0.134 \times 500}{2(0.9570)} + \frac{3}{2} = 35.004 + 1.5 = 36.5 \text{ m}$$

SP 428:

$$d_w = \frac{0.135 \times 500}{2(0.9570)} + \frac{3}{2} = 35.266 + 1.5 = 36.77 \text{ m}$$

SP 430:

$$d_w = \frac{0.137 \times 500}{2(0.9570)} + \frac{3}{2} = 35.789 + 1.5 = 37.29 \text{ m}$$

SP 500:

$$d_w = \frac{0.189 \times 500}{2(0.9570)} + \frac{3}{2} = 49.372 + 1.5 = 50.87 \text{ m}$$

DISCUSSION

From the result obtained a procedure to determine weathering trend along a seismic line using reflection data has been dealt with, using data from LINE 105, OML 39 of the Okuibome Prospect (Delta State) South West of Niger Delta Basin as case study. The weathering velocity for this work was supplied from an uphole survey in the area. Using the slope of the best curve of the different plots of first break time against the take off distance of the traces, the elevation velocity of the different shot point at given shot elevation was obtained. The elevation velocity obtained ranges from 1642 ms^{-1} western part of the field to 1862 ms^{-1} eastern part of the field, with an average elevation velocity of 1724 ms^{-1} across field line. A datum surface was then assumed for both the shot and geophones elevations which is used to calculate the surface elevation of the shot and geophone points, this plots gives the surface topography of the study area. The elevation velocities obtained, shot depth, instrument delay and the calculated modified intercept time T_{mod} were substituted into equation 7 and 8 (given earlier) to obtain the weathering depth along the shot point and geophone point along the line. The weathering depth obtained ranges from 35.46m in the low side (western part) of field to 50.87m in the high side (eastern part) (Table 5), with an average of 42.66m across the line. A plot of the calculated weathering depth along the W-E orientation of the field at each shot point (SP 422-500) was then plotted above the shot and geophone elevations to delineate the weathering trend of the study area. The variation of the weathering thickness obtained along the seismic line was found to be significant. From the result obtained for both the weathering thickness and the topography when plotted on the same scale shows that the weathering thickness along the line is directly affected by the shot and the geophone elevation respectively (surface topography), because the higher the topography of the shot and geophone from the datum the bigger the

weathering thickness. Thus the weathering thickness is topography dependent.

The determination of weathering trend, especially from reflection data is an important aspect of petroleum exploration, not only does it help in making decision on improved quality of data acquired, it also helps in the subsequent processing of the data where statics have to be computed for every shot and receiver station. Determination of weathering trend from uphole survey may not give an accurate representation of the trend since such survey is too costly to be carried out at every shot point along a seismic line and so a lot of interpolations will have to be made to delineate the weathering trend.

Weathering trend determination is also an important tool in engineering. With overburden thickness accurately known at short distances along a survey line, a good decision could be made regarding suitable sites for engineering constructions.

Therefore, for accurate weathering trend determination in a prospect area to be made using seismic data, industries should resort to the use of seismic reflection data (instead of the common uphole survey technique) since accurate weathering thickness could be determined at shorter distances.

REFERENCES

- Coffeen, J.A.** (1978), "Seismic Exploration Fundamentals", Petro Publishing Co, Tulsa
- Bridle, R., Ley, R., Al-Mustafa, A.,** (2007), "Near Surface Model in Saudi Arabia" Geophysical Prospecting, Vol 55, Issue 6, pp779-797
- Dobrin, M.B.** (1976), "Introduction to Geophysical Prospecting", McGraw Hill Publishing, New York
- Hampson, D., Russell, B.,** (1984), "First Break Interpretation Using Generalized Linear

- Inversion”, Journal of the Canadian Society of Exploration Geophysicists, Vol. 20, No1, pp 40-54
- Hubral, P., Krey, T.** (1980), “Determination of Internal Velocities from Seismic time measurement”, SEG Publ., Tulsa
- May, B.T., Covey, J.D.**, (1981), “Inverse Method for Computing Geologic Structures from Seismic Reflections, Zero-off set case”, Geophysics 46, pp 268-287
- NNPC - IDSL** (1992), Interpretation manual on seismic data reductions.
- Sheriff, R.E.** (1978), “First course in Geophysical Exploration and Interpretation”, IHRDC Publishing, Boston
- Sheriff, R.E.** (2006), “Encyclopedic Dictionary of Applied Geophysics – 4th Ed
- Telford, W., Geldart, L.P., Sheriff, R.E., Keys, D.A.** (1982), “Applied Geophysics: Cambridge University Press, New York,
- Toksovet, J.** (1982). “Seismic Exploration: McGraw Encyclopedia of Science and Technology, Vol. 16.
- Waters, K.H.** (1978), “Reflection Seismology; A tool for Energy Resource Exploration”, Wiley Publishing, New York
- Whiteman, A.** (1982), “Nigeria: Petroleum Geology, Resources and Potential”, Graham and Trotman Publishing, London.
- Yilmaz, Oz.**, (2001), “Seismic Data Analysis: Processing, Inversion and Interpretation of Seismic Data, Vol 1.